iScience

CellPress
OPEN ACCESS

Article

KLHL7 promotes hepatocellular carcinoma progression and molecular therapy resistance by degrading RASA2

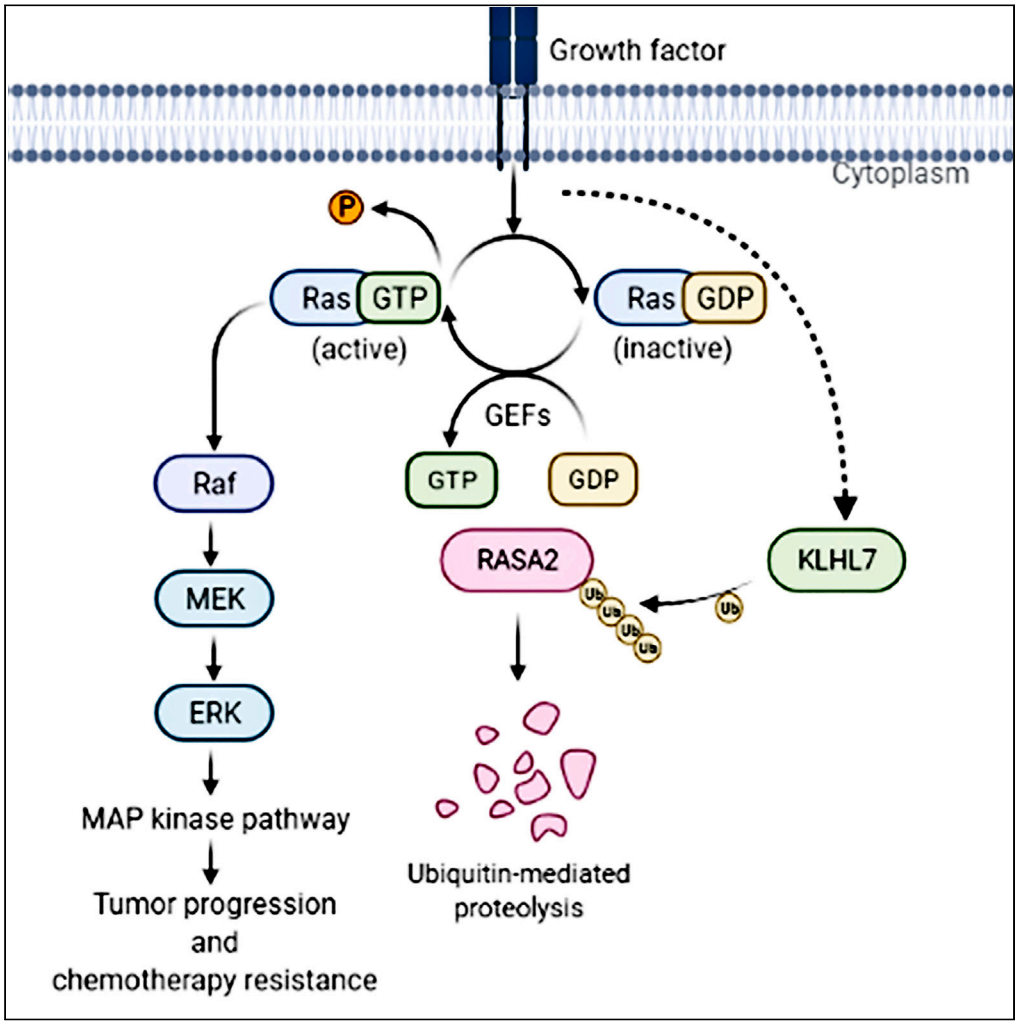

Lin Chen, Yun Li, Yongheng Chen

yonghenc@csu.edu.cn

Highlights

KLHL7 acts as an oncogene in hepatocellular carcinoma

KLHL7 enhances RAS-MAPK signaling pathway

KLHL7 promotes polyubiquitination and degradation of RASA2

Inhibition of KLHL7 increases the efficacy of lenvatinib

Chen et al., iScience 26, 106914
June 16, 2023
https://doi.org/10.1016/j.isci.2023.106914

iScience

CellPress
OPEN ACCESS

Article

KLHL7 promotes hepatocellular carcinoma progression and molecular therapy resistance by degrading RASA2

Lin Chen,[1] Yun Li,[1] and Yongheng Chen[1,2,*]

SUMMARY

Hepatocellular carcinoma (HCC) is a common aggressive tumor with a poor prognosis, and patients often seem to be refractory to the use of therapeutic drugs. In this study, we found that the KLHL7 expression was upregulated in HCC that was associated with poor patient prognosis. KLHL7 has been found to promote HCC development in both *in vitro* and *in vivo* experiments. Mechanistically, RASA2, a RAS GAP, was identified as a substrate of KLHL7. Upregulation of KLHL7 by growth factors promotes K48-linked polyubiquitination of RASA2 for degradation via the proteasomal pathway. Our *in vivo* experiments revealed that inhibition of KLHL7 in combination with lenvatinib treatment resulted in efficient killing of HCC cells. Together, these findings demonstrate a role for KLHL7 in HCC and reveal a mechanism by which growth factors regulate the RAS-MAPK pathway. It represents a potential therapeutic target for HCC.

INTRODUCTION

Hepatocellular carcinoma (HCC) is the world's leading cause of cancer-related death and accounts for 85%–90% of liver malignancies. Because of rapid hepatocellular progression, 80% of patients are unsuitable for surgical intervention. As a result, the majority of patients with HCC receive systemic drug therapy.[1] However, the exact etiology and molecular mechanism of primary HCC is not fully understood. This partly explains the failure of numerous clinical trials of new drugs.[2–4] The first-line therapy for advanced HCC is a combination of the immune checkpoint inhibitor atezolizumab and the VEGF inhibitor bevacizumab.[5] However, sorafenib and lenvatinib are still widely used in clinical practice. Both are multikinase inhibitors that simultaneously inhibit VEGFR, PDGFR, FGFR, and other receptor tyrosine kinases.[6,7]

As the primary downstream RTK signaling pathway, the RAS-MAPK signaling pathway is an important target of both sorafenib and lenvatinib.[8,9] This highlights the significance of the RAS-MAPK signaling pathway in HCC.[10,11] RAS is a small GTPase that binds to GTP and hydrolyzes it to GDP, and GTP-bound RAS can stimulate downstream signal transduction. Therefore, it is very important to regulate the GTP status of RAS. The interaction between RAS and GTP is regulated by guanine nucleotide exchange factors (GEFs) and GTPase activating proteins (GAPs). The former converts RAS-bound GDP to GTP, activating the downstream effectors. The latter promotes GTP hydrolysis to GDP, thereby turning RAS off.[12,13] In addition to activating mutations in RAS proteins, inactivating mutations in GAPs have also been reported to promote tumorigenesis in tumors, with NF1, SPRED1, RASA1, and RASA2 being the most significant.[14–18]

KLHL7 is an integral component of the BCR (BTB-CUL3-RBX1) E3 ubiquitination ligase system and is primarily involved in the specific recognition of substrates.[19,20] Previous studies have shown that KLHL7 regulates the modification of the K48-linked ubiquitination chain, which is primarily involved in the proteasomal degradation of target proteins.[21] Clinically, germline mutations in KLHL7 can cause degenerative disorders such as retinitis pigmentosa and Perching's syndrome.[21,22] So far, few studies have reported the role of KLHL7 in cancer, and its role in HCC is unclear.

In this study, we found that KLHL7 degrades RASA2, a RAS GAP. Increased expression of KLHL7 in HCC was associated with poor prognosis. KLHL7 promotes tumor progression and drug resistance by modulating the RAS-MAPK signaling pathway.

[1]Department of Oncology, NHC Key Laboratory of Cancer Proteomics, State Local Joint Engineering Laboratory for Anticancer Drugs, National Clinical Research Center for Geriatric Disorders, Xiangya Hospital, Central South University, Changsha, Hunan 410008, China

[2]Lead contact

*Correspondence: yonghenc@csu.edu.cn

https://doi.org/10.1016/j.isci.2023.106914

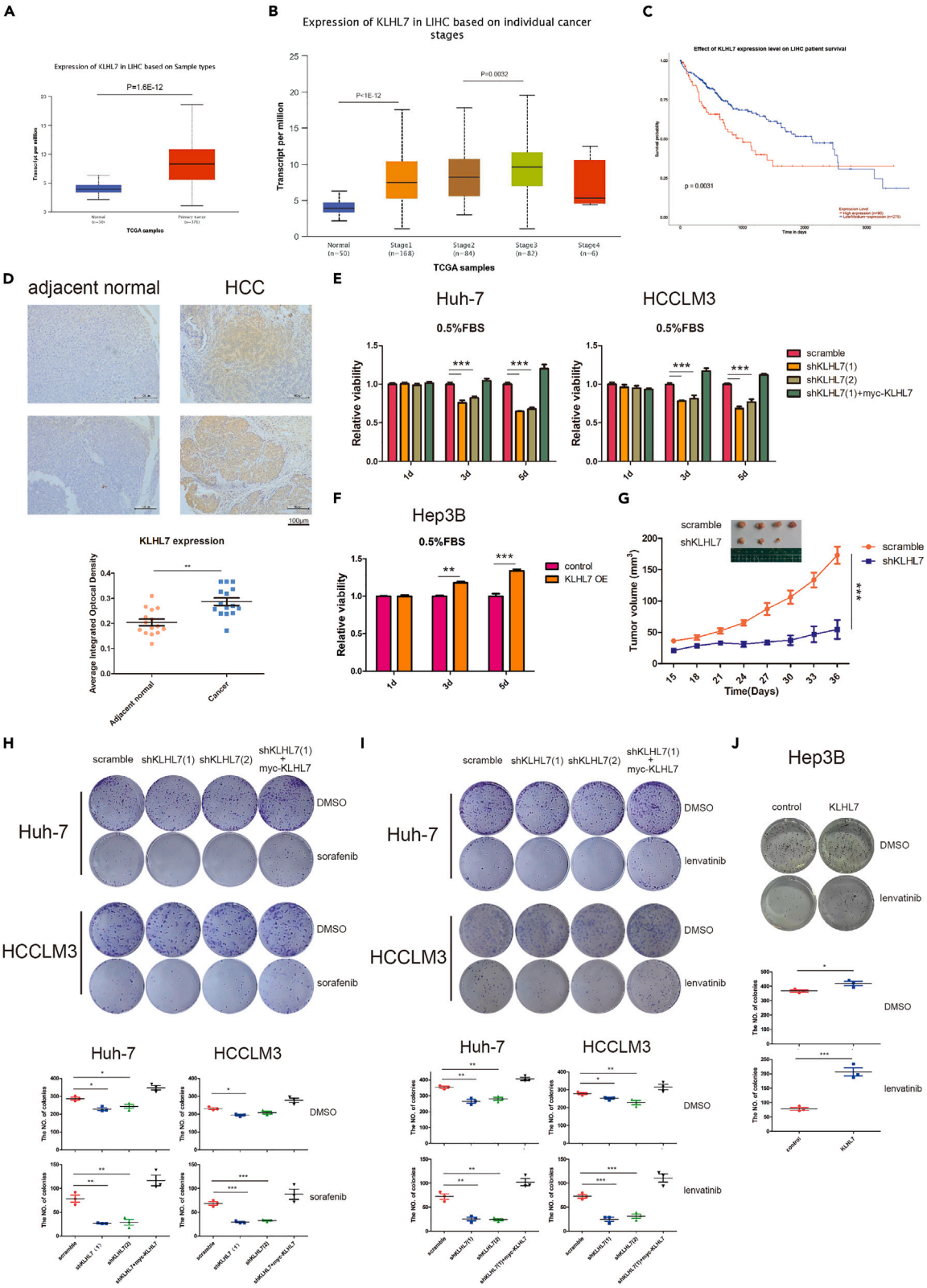
A
Expression of KLHL7 in LIHC based on Sample types
P=1.6E-12
Transcript per million
TCGA samples
B
Expression of KLHL7 in LIHC based on individual cancer stages
P<1E-12
P=0.0032
Transcript per million
Normal (n=50)
Stage1 (n=168)
Stage2 (n=84)
Stage3 (n=82)
Stage4 (n=6)
TCGA samples
C
Effect of KLHL7 expression level on LIHC patient survival
p = 0.0031
Survival probability
Time in days
D
adjacent normal
HCC
100μm
KLHL7 expression
Average Integrated Optocal Density
Adjacent normal
Cancer
E
Huh-7
0.5%FBS
HCCLM3
0.5%FBS
Relative viability
1d
3d
5d
scramble
shKLHL7(1)
shKLHL7(2)
shKLHL7(1)+myc-KLHL7
F
Hep3B
0.5%FBS
Relative viability
control
KLHL7 OE
G
scramble
shKLHL7
Tumor volume (mm3)
Time(Days)
H
scramble
shKLHL7(1)
shKLHL7(2)
shKLHL7(1) + myc-KLHL7
Huh-7
HCCLM3
DMSO
sorafenib
The NO. of colonies
I
scramble
shKLHL7(1)
shKLHL7(2)
shKLHL7(1) + myc-KLHL7
Huh-7
HCCLM3
DMSO
lenvatinib
J
Hep3B
control
KLHL7
DMSO
lenvatinib
The NO. of colonies

Figure 1. KLHL7 is upregulated and promotes tumor proliferation and resistance to chemotherapy in hepatocellular carcinoma

(A) KLHL7 mRNA expression in normal liver tissue and primary tumors (data from TCGA, ualcan.path.uab.edu).

(B) KLHL7 mRNA expression in different stages of HCC (data from TCGA).

(C) Overall survival curve of HCC patients with high and low/medium KLHL7 mRNA expression (data from TCGA, ualcan.path.uab.edu).

(D) Immunohistochemical images of KLHL7 in adjacent and cancerous tissues. Image magnification is 20×. Scale bar, 100 μm. The average optical density of 15 pairs of tissues is displayed at the bottom. Data are the mean ± s.e.m. n = 15. Significance was determined using a paired t test. $^{**}p < 0.01$.

(E) Cell viability of Huh-7 and HCCLM3 cell lines after KLHL7 knockdown under low serum (0.5% FBS) culture conditions. Cell numbers were calculated by adding CCK-8 and measuring the absorbance at 450 nM. Data are the mean ± s.e.m. n = 4. Significance was determined using Student's *t* test. $^{**}p < 0.01$, $^{***}p < 0.001$.

(F) Viability of Hep3B cells after exogenous KLHL7 expression under low serum (0.5% FBS) culture conditions. Cell numbers were calculated by adding CCK-8 and measuring the absorbance at 450 nM. Data are the mean ± s.e.m. n = 4. Significance was determined using Student's *t* test. $^{**}p < 0.01$, $^{***}p < 0.001$.

(G) Proliferation curve of Huh-7 cells following KLHL7 knockdown *in vivo*. Tumor volume is displayed by physical photos (top) and tumor measurements (bottom). Data are the mean ± s.e.m. n = 3. Significance was determined using Student's *t* test. $^{***}p < 0.001$.

(H) Colony formation was assessed in scramble and shKLHL7 cells after 2 weeks of sorafenib treatment under normal serum (10% FBS) culture conditions. Statistics on the number of remaining clones are shown at the bottom. The sorafenib concentrations were 2.5 μM (Huh-7) and 5 μM (HCCLM3). Data are the mean ± s.e.m. n = 3. Significance was determined using Student's *t* test. $^{*}p < 0.05$, $^{**}p < 0.01$, $^{***}p < 0.001$.

(I) Colony formation was assessed in scramble and shKLHL7 cells after 2 weeks of lenvatinib treatment under normal serum (10% FBS) culture conditions. The statistics of the number of remaining clones are displayed at the bottom. Lenvatinib concentrations were 0.5 μM (Huh-7) and 1 μM (HCCLM3). The data are the mean ± s.e.m. n = 3. Student's *t* test was used to establish significance.$^{*}p < 0.05$, $^{**}p < 0.01$, $^{***}p < 0.001$.

(J) Colony formation was assessed in control and exogenous KLHL7 expression Hep3B cells after two weeks of lenvatinib treatment under normal serum (10% FBS) culture conditions. The statistics of the number of remaining clones are displayed at the bottom. The lenvatinib concentration was 0.5 μM. The data are the mean ± s.e.m. n = 3. Student's *t* test was used to establish significance.$^{*}p < 0.05$, $^{***}p < 0.001$.

RESULTS

KLHL7 acts as an oncogene in hepatocellular carcinoma

The role of the E3 ubiquitination ligase KLHL7 in HCC is unclear. To explore its role in HCC, we analyzed the public databases to determine KLHL7 expression in HCC and its impact on patient prognosis.[23–25] Results showed a significant increase in KLHL7 expression in HCC tissues compared to normal tissues (Figure 1A), and its expression was upregulated with the stage of HCC (Figure 1B). Furthermore, increased KLHL7 expression was associated with poor overall survival and worse progression-free survival (Figures 1C and S1A). In our immunohistochemistry analysis, KLHL7 expression was found to be higher in cancerous tissues compared to adjacent normal tissues (Figure 1D). These findings suggest that KLHL7 is an oncogene in HCC.

To test this hypothesis, we first examined the effect of KLHL7 on hepatoma cell viability. Considering that KLHL7 was highly expressed in Huh-7 and HCCLM3 cells (Figure S1B), we decided to knockdown KLHL7 in both cell lines in order to observe the effect of KLHL7 on HCC. We observed inhibition of cell viability in Huh-7 and HCCLM3 cell lines following KLHL7 knockdown, especially under culture conditions of low serum concentration (0.5% FBS) (Figures 1E and S1C). Meanwhile, the inhibitory effects of KLHL7 knockdown were reversed by exogenous KLHL7 expression (Figures 1E and S1C). It ruled out shRNA-induced off-target effects. In addition, in the Hep3B cell line with relatively low levels of KLHL7, exogenous expression of KLHL7 increased cell viability in low serum culture conditions (Figures 1F and S1D).

Low serum concentrations often indicate low growth factor levels.[26,27] Growth factor signaling via receptor tyrosine kinases is the main mechanism of the current first line targeted therapy agents for HCC, sorafenib and lenvatinib.[11] This, coupled with the above clinical data results, allowed us to investigate the role of KLHL7 in the molecular treatment of the HCC under normal serum (10% FBS) culture conditions. KLHL7 knockdown was carried out by two different shRNAs in Huh-7 and HCCLM3 cell lines followed by treatment with lenvatinib for colony formation assays. The results demonstrated that when KLHL7 expression was inhibited, the number of clones formed by the cells was significantly reduced, and this effect could be reversed by exogenous KLHL7 expression (Figure 1I). A similar result was obtained from experiments with another molecular therapy drug, sorafenib, in which the combination of KLHL7 knockdown with sorafenib treatment significantly inhibited the proliferation of the HCC cell lines (Figure 1H). In addition, the resistance of Hep3B cells to lenvatinib was dramatically increased following expression of exogenous KLHL7 (Figure 1J). These findings suggest that KLHL7 promotes HCC cell resistance to molecular therapy drugs.

We further evaluated the role of KLHL7 in tumorigenesis. *In vivo*, KLHL7 knockdown significantly inhibited subcutaneous xenograft tumor growth in immune-deficient mice (Figure 1G). Therefore, these results are adequate to demonstrate that KLHL7 is an oncogene in HCC.

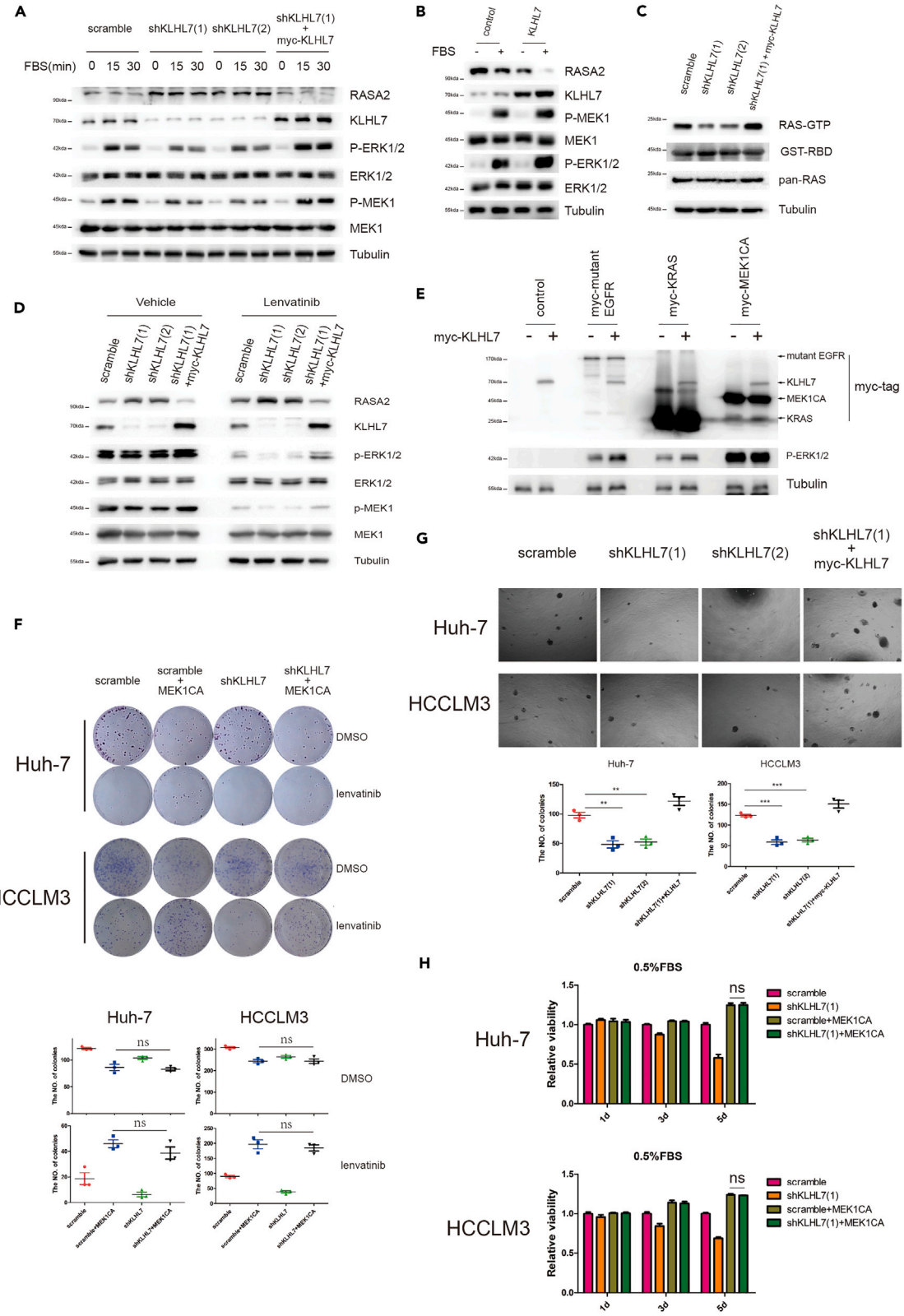
A
scramble
shKLHL7(1)
shKLHL7(2)
shKLHL7(1) + myc-KLHL7
FBS(min) 0 15 30 0 15 30 0 15 30 0 15 30
RASA2
KLHL7
P-ERK1/2
ERK1/2
P-MEK1
MEK1
Tubulin
B
control
KLHL7
FBS - + - +
RASA2
KLHL7
P-MEK1
MEK1
P-ERK1/2
ERK1/2
Tubulin
C
scramble
shKLHL7(1)
shKLHL7(2)
shKLHL7(1) + myc-KLHL7
RAS-GTP
GST-RBD
pan-RAS
Tubulin
D
Vehicle
Lenvatinib
scramble
shKLHL7(1)
shKLHL7(2)
shKLHL7(1) +myc-KLHL7
RASA2
KLHL7
p-ERK1/2
ERK1/2
p-MEK1
MEK1
Tubulin
E
control
myc-mutant EGFR
myc-KRAS
myc-MEK1CA
myc-KLHL7 - + - + - + - +
mutant EGFR
KLHL7
MEK1CA
KRAS
myc-tag
P-ERK1/2
Tubulin
F
scramble
scramble + MEK1CA
shKLHL7
shKLHL7 + MEK1CA
Huh-7
HCCLM3
DMSO
lenvatinib
Huh-7
HCCLM3
ns
The NO. of colonies
scramble
scramble+MEK1CA
shKLHL7
shKLHL7+MEK1CA
G
scramble
shKLHL7(1)
shKLHL7(2)
shKLHL7(1) + myc-KLHL7
Huh-7
HCCLM3
Huh-7
HCCLM3
The NO. of colonies
scramble
shKLHL7(1)
shKLHL7(2)
shKLHL7(1)+KLHL7
shKLHL7(1)+myc-KLHL7
H
0.5%FBS
Huh-7
HCCLM3
Relative viability
ns
scramble
shKLHL7(1)
scramble+MEK1CA
shKLHL7(1)+MEK1CA
1d
3d
5d

Figure 2. KLHL7 upregulates the RAS-MAPK pathway and promotes resistance to chemotherapy

(A) Serum-starved KLHL7 knockdown and control Huh-7 cells were treated with fetal bovine serum (FBS) for the indicated times before being lysed for immunoblotting. Western blotting was used to detect the expression of the indicated proteins.

(B) Serum-starved KLHL7 knockdown and control Huh-7 cells were treated with fetal bovine serum (FBS) for the indicated times before being lysed for immunoblotting. Western blotting was used to detect the expression of the indicated proteins.

(C) GTP-bound RAS in Huh-7 cells. Serum-starved KLHL7 knockdown and control Huh-7 cells were stimulated with fetal bovine serum (FBS) for 5 min and lysed for GST-RAS-RBD pulldown. The pulldown protein was detected by immunoblotting.

(D) KLHL7 knockdown and control Huh-7 cells were treated with lenvatinib (5 μM) for 2 h and lysed for immunoblotting. Western blotting was used to detect the expression of the indicated proteins.

(E) 293T cells were transfected with the indicated genes and lysed for immunoblotting. Western blotting detected the expression of the indicated proteins.

(F) Colony formation assays were performed with scramble and shKLHL7 Huh-7 cells transfected with or without MEK1CA after 2 weeks of lenvatinib treatment. Statistics on the number of remaining clones are shown at the bottom. Lenvatinib concentrations were 0.5 μM (Huh-7) and 1 μM (HCCLM3). Data are the mean ± s.e.m. n = 3. Significance was determined using Student's *t* test. ns $p > 0.05$.

(G) A soft agar formation assay was performed with KLHL7 knockdown and control cells. Data are the mean ± s.e.m. n = 3. Significance was determined using Student's *t* test. **$p < 0.01$, ***$p < 0.001$.

(H) Cell viability assays were performed using scramble and shKLHL7 Huh-7 and HCCLM3 cells transfected with or without MEK1CA in media containing 0.5% fetal bovine serum. The cell number was detected by adding CCK-8 and measuring the absorbance at 450 nM. Data are the mean ± s.e.m. n = 4. Significance was determined using Student's *t* test. ns $p > 0.05$.

KLHL7 enhances RAS-MAPK signaling pathway activation

We then sought to determine the mechanism by which KLHL7 promotes tumorigenesis and therapeutic resistance in HCC. Considering the importance of the RAS-MAPK signaling pathway as a target for molecular therapeutics and the fact that the protein interaction database (bioplex.hms.harvard.edu) suggesting that KLHL7 can interact directly with RASA2, a RAS GAP (Figure 3A), the effect of KLHL7 on the RAS-MAPK signaling pathway was investigated. Immunoblotting revealed that KLHL7 knockdown in Huh-7 and HCCLM3 cells inhibited the phosphorylation of ERK1/2 and MEK1 following serum stimulation (Figures 2A and S2A). KLHL7 overexpression also significantly increased ERK1/2 and MEK1 phosphorylation in the Hep3B cell line as well (Figure 2B). We then enriched GTP-bound RAS to determine the effect of KLHL7 on RAS activity through GST-RAF1-RBD pulldown.[28,29] GTP-bound RAS was significantly reduced after KLHL7 knockdown (Figure 2C). These findings indicate that KLHL7 can contribute to the positive regulation of the RAS-MAPK signaling pathway. It is well established that the RAS-MAPK signaling pathway is critical for the anchorage-independent growth of tumors.[30] Consistent with this finding, KLHL7 knockdown significantly inhibited the clonogenicity of cancer cells, as demonstrated by a soft agar formation assay (Figure 2G).

Next, we examined whether KLHL7 promotes tumorigenesis and resistance to therapy in HCC cells through the RAS-MAPK signaling pathway. Indeed, lenvatinib inhibited the phosphorylation of ERK1/2 and MEK1 in HCC cells, and this inhibition was more pronounced upon further KLHL7 knockdown (Figure 2D). Following exogenous KLHL7 expression, we were able to recover the levels of ERK1/2 and MEK1 phosphorylation (Figure 2D). Furthermore, we investigated whether MAPK reactivation could rescue the increased therapeutic sensitivity induced by KLHL7 knockdown. We found that the cytotoxicity of lenvatinib was significantly reduced following the introduction of constitutively activated MEK1 (MEK1CA),[31,32] meanwhile KLHL7 knockdown did not further improve the sensitivity of Huh-7 and HCCLM3 cells to lenvatinib following MEK1CA expression (Figure 2F). Similarly, the reduction in cell viability induced by KLHL7 knockdown was ameliorated by the introduction of constitutively activated MEK1 (Figures 2H and S2B). In conclusion, these results demonstrated that KLHL7 promoted HCC proliferation and resistance to molecular therapy by upregulating the RAS-MAPK signaling pathway.

KLHL7 promotes polyubiquitination and degradation of RASA2

As a component of the BCR (BTB-CUL3-RBX1) E3 ubiquitination ligase system, KLHL7 is primarily involved in K-48-linked polyubiquitination, which plays an important role in proteasomal degradation of target proteins.[21,33] Therefore, KLHL7 may be involved in the degradation of proteins that negatively regulate the RAS-MAPK signaling pathway. To determine the role of KLHL7 in the RAS-MAPK pathway, we activated it at different sites. We observed that in 293T cells with constitutively activated MEK1CA overexpression, overexpression of KLHL7 did not further affect the phosphorylated ERK1/2 (Figure 2E). In contrast, KLHL7 overexpression could still improve phosphorylated ERK1/2 after KRAS or active mutant EGFR overexpression (Figure 2E). Given that KLHL7 can promote GTP binding to RAS (Figure 2C), RAS GAPs became the logical target for KLHL7. Moreover, the bioplex protein interaction database,[34,35] revealed that KLHL7 interacts with RASA2, which was verified in our Co-IP experiments (Figures 3A, 3C, S3A, and S3D). This interaction was also verified by immunofluorescent

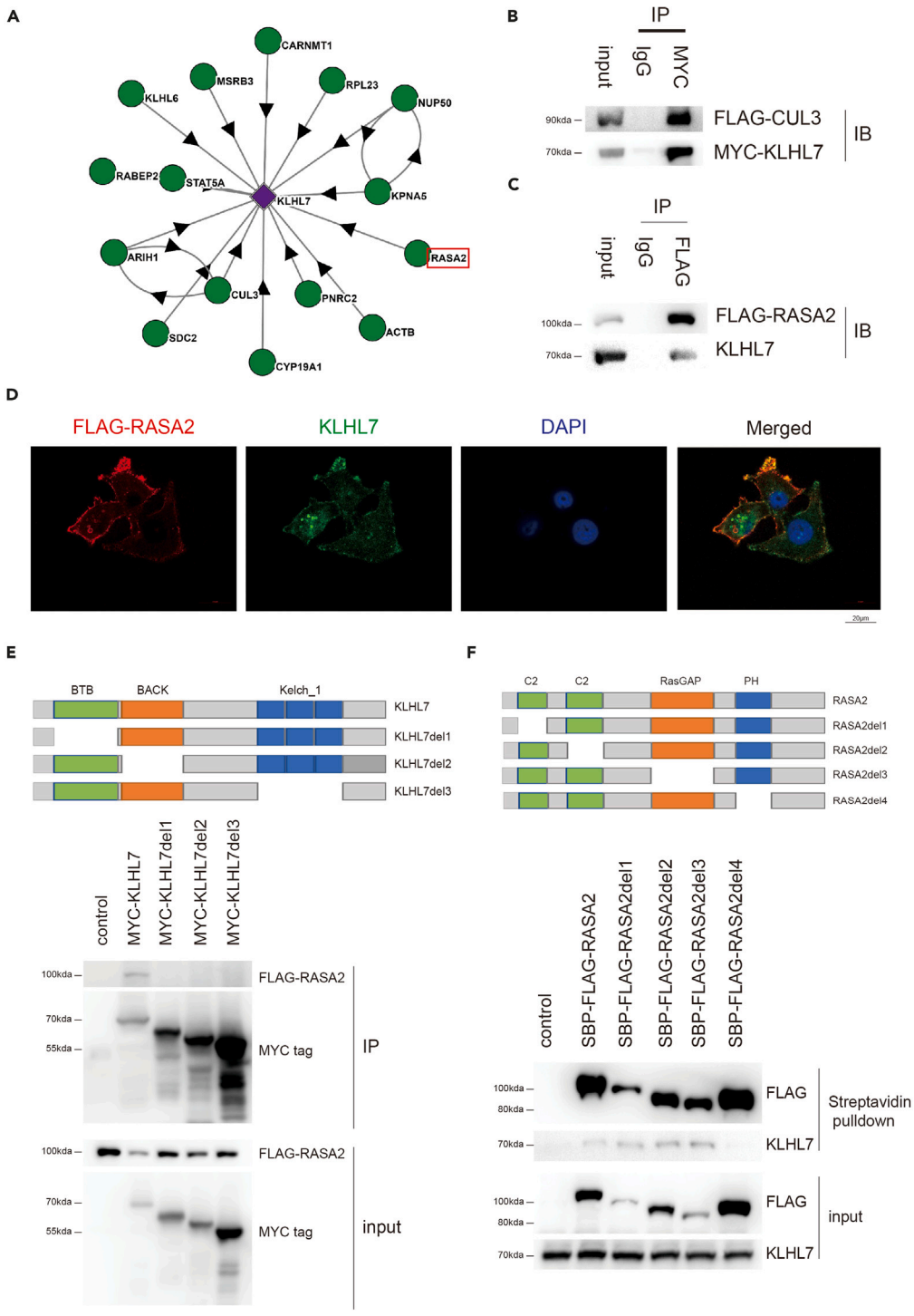

Figure 3. KLHL7 interacts with RASA2

(A) Proteins that interact with KLHL7. Data provided by Bioplex.

(B) 293T cells were transfected with Flag-tagged CUL3 and Myc-tagged CUL3. Cells were lysed for coimmunoprecipitation with an anti-Myc antibody. Whole-cell lysis and protein precipitation were detected by immunoblotting.

(C) Huh-7 cells were transfected with Flag-tagged RASA2 and lysed for coimmunoprecipitation with an anti-Flag antibody. Whole-cell lysis and protein precipitation were detected by immunoblotting.

Figure 3. *Continued*

(D) HCCLM3 cells were transfected with exogenous FLAG-RASA2. Cells were treated with MG132 (10 μM) for 8 h and then stained by immunofluorescence. Fluorescence showed FLAG-RASA2 (red) and KLHL7 (green). Cell nuclei were stained with DAPI(blue). Scale bar, 20 μm.

(E) 293T cells were cotransfected with Flag-tagged RASA2 and mutant MYC-tagged KLHL7, lysed and immunoprecipitated. Whole-cell lysis and protein precipitation were detected by immunoblotting.

(F) 293T cells were cotransfected with mutant Flag-tagged RASA2 and MYC-tagged KLHL7, lysed, and subjected to streptavidin bead pulldown. Whole-cell lysis and protein precipitation were detected by immunoblotting.

staining. Endogenous KLHL7 and ectopically expressed FLAG-tagged RASA2 showed overlapping cell immunostaining (Figure 3D). Then, we examined the effect of KLHL7 on RAS GAP expression. After 293T exogenous expressed various RAS GAPs alone or in combination with KLHL7, immunoblotting revealed that KLHL7 primarily inhibited the expression of RASA2 and, and MG-132, a proteasome inhibitor, reversed this inhibition (Figures 4A, S3B, and S3C). Moreover, KLHL7 knockdown increased the expression of RASA2 in Huh-7 cells, but this increase was abolished following the addition of the proteasome inhibitor MG-132 (Figure 4B). Meanwhile, the mRNA levels of RASA2 remained unchanged (Figure S2C). We also investigated the effect of KLHL7 on the protein stability of RASA2 and KLHL7 knockdown significantly decreased the rate of degradation of RASA2 protein in Huh-7 cells treated with CHX to inhibit translation (Figure 4C).

Next, we determined whether KLHL7-induced RASA2 degradation was a result of ubiquitination. We coexpressed SBP[36] and FLAG-tagged RASA2 along with wild-type or mutant HA-tagged ubiquitin[37] in 293T cells. Purification of RASA2 using streptavidin beads revealed that KLHL7 significantly increased RASA2 ubiquitination (Figure 4D). Similar results were also observed when expressing HA-tagged ubiquitin with only K48 and other lysines mutated to arginines but not with only K63 and other lysines mutated to arginines (Figure 4D). These findings support our hypothesis that KLHL7 promotes RASA2 K48-linked ubiquitination and proteasome-mediated degradation.

Subsequently, expression vectors encoding different mutants of KLHL7 and RASA2 were transfected into 293T cells to determine the domain that was involved in the interaction of KLHL7 and RASA2. KLHL7 functions as an adapter for the BCR (BTB-CUL3-RBX1) ubiquitination ligase. Its BTB and RACK domains form dimerization and bind to CUL3, which is important for substrate binding, whereas the Kelch domain is responsible for direct binding to the substrate.[38,39] As expected, KLHL7 was unable to bind RASA2 after the deletion of either domain (Figure 3E). We also deleted the domains of RASA2 separately, and the results indicate that the RASA2 protein's PH domain is crucial for binding to KLHL7 (Figure 3F).

Interestingly, serum stimulation after cell starvation resulted in increased KLHL7 expression and decreased RASA2 expression (Figures 2A and S2A). These changes in KLHL7 and RASA2 occurred at the posttranscriptional level because their mRNA levels were unaltered (Figure S2D). As the expression of KLHL7 increased after serum stimulation, more KLHL7 was bound to RASA2, which induced more RASA2 degradation (Figure 4E). We also examined the level of RASA2 ubiquitination after serum stimulation. Serum stimulation induced an increase in RASA2 ubiquitination, which was impaired by KLHL7 knockdown (Figure 4F). These findings indicate that growth factor-induced KLHL7 may represent a regulatory approach to promote the activation of RAS-MAPK signaling.

KLHL7 promotes tumorigenesis and resistance to therapy via RASA2

We next sought to determine if KLHL7 promotes hepatocarcinogenesis and chemotherapeutic drug resistance by degrading RASA2.

First, we investigated whether RASA2 mediated the regulatory effects of KLHL7 on the RAS-MAPK signaling pathway. The results revealed that RASA2 knockdown in Huh-7 and HCCLM3 cells increased the phosphorylation of MEK1 and ERK1/2 and also the GTP-bound RAS, whereas further KLHL7 knockdown had no significant effect on these indicators following RASA2 knockdown (Figures 5A, 5B, and S4A). We further performed gain of function experiments in KLHL7 low expressing Hep3B cells. Expression of exogenous KLHL7 increased MAPK activity, which was significantly inhibited by further expression of RASA2 (Figure S4C).

We then investigated whether KLHL7 promoted the viability of hepatoma cells via RASA2. Following RASA2 knockdown, the inhibitory effect of KLHL7 knockdown on cell viability was attenuated (Figures 5C and S4B). In Hep3B cells, the exogenous expression of KLHL7 was shown to significantly increase cell viability, and further exogenous RASA2 expression significantly decreased the viability of cells

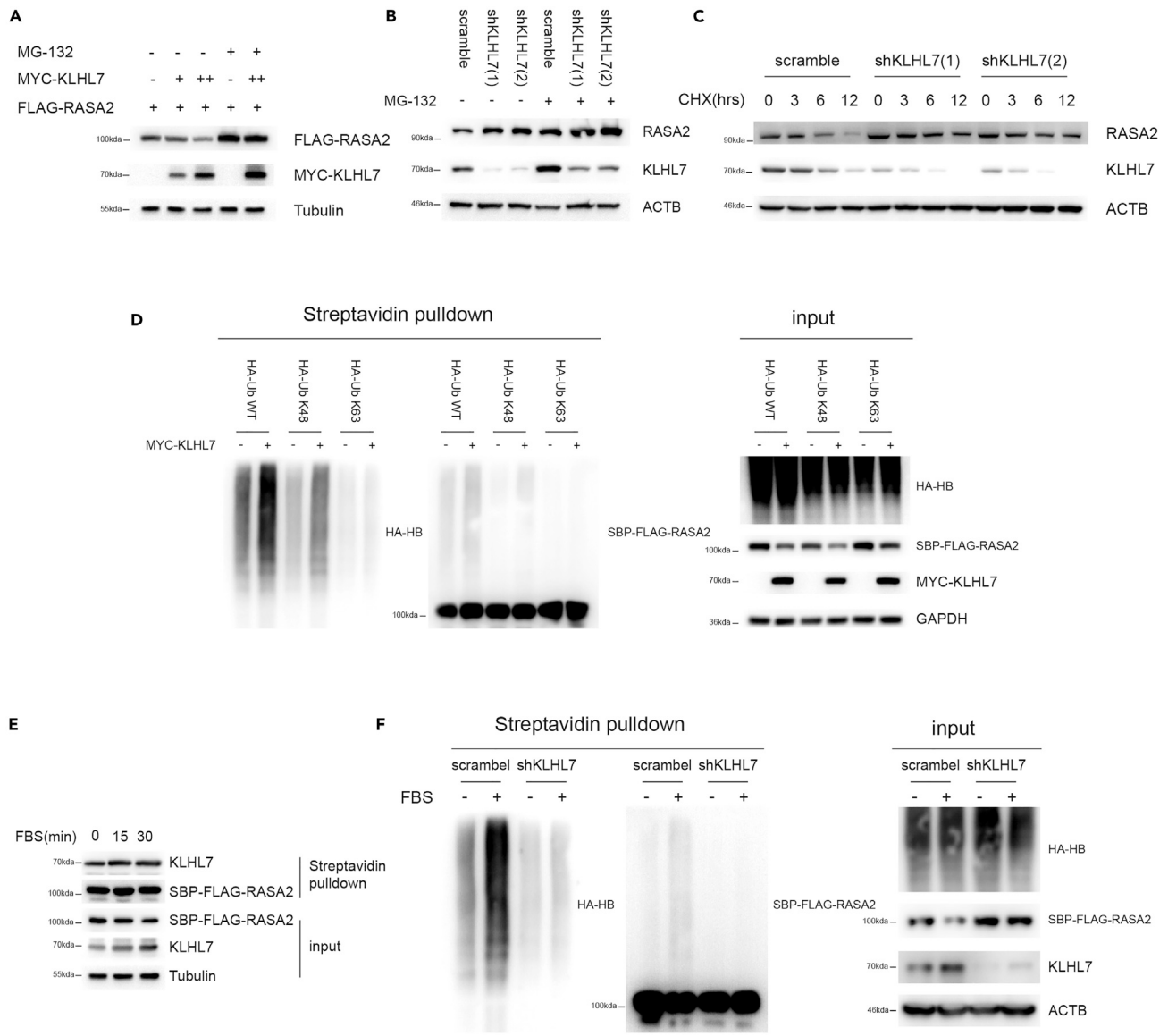

Figure 4. KLHL7 ubiquitinates and degrades RASA2

(A) 293T cells were transfected with RASA2 with or without KLHL7. After 16 h of n-k48 (10 μM) treatment, the cells were lysed and used for immunoblotting.

(B) KLHL7 knockdown and control Huh-7 cells were treated with vehicle or MG-132 (10 μM). Whole-cell lysates were collected and immunoblotted.

(C) KLHL7 knockdown and control Huh-7 cells were treated with either vehicle or CHX. Whole-cell lysates were collected, and immunoblotting was performed.

(D) 293T cells were cotransfected with mutant Flag-tagged RASA2 and HA-tagged ubiquitin with and without Myc-tagged KLHL7, lysed, and subjected to streptavidin bead pulldown. Whole-cell lysis and protein precipitation were detected by immunoblotting.

(E) Huh-7 cells were transfected with SBP-Flag-tagged RASA2, serum-deprived for 16 h before being triggered with FBS for 15 min and lysed for streptavidin bead pulldown. Whole-cell lysis and protein precipitation were detected by immunoblotting.

(F) 293T cells were cotransfected with SBP-Flag-tagged RASA2 and HA-tagged ubiquitin with and without shKLHL7. Cells were deprived of serum for 16 h before being triggered with FBS for 15 min and lysed for streptavidin bead pulldown. Whole-cell lysis and protein precipitation were detected by immunoblotting.

(Figure S4D). Subsequently, we investigated whether KLHL7 promotes anchorage-independent growth in an RASA2-dependent manner using soft agar colony formation assays. The results indicated that the number of clones formed by the simultaneous knockdown of RASA2 and KLHL7 was not significantly different from the number of clones formed by downregulation of RASA2 alone (Figure 5D). Therefore, we demonstrated *in vitro* that KLHL7 promoted tumorigenesis primarily via RASA2.

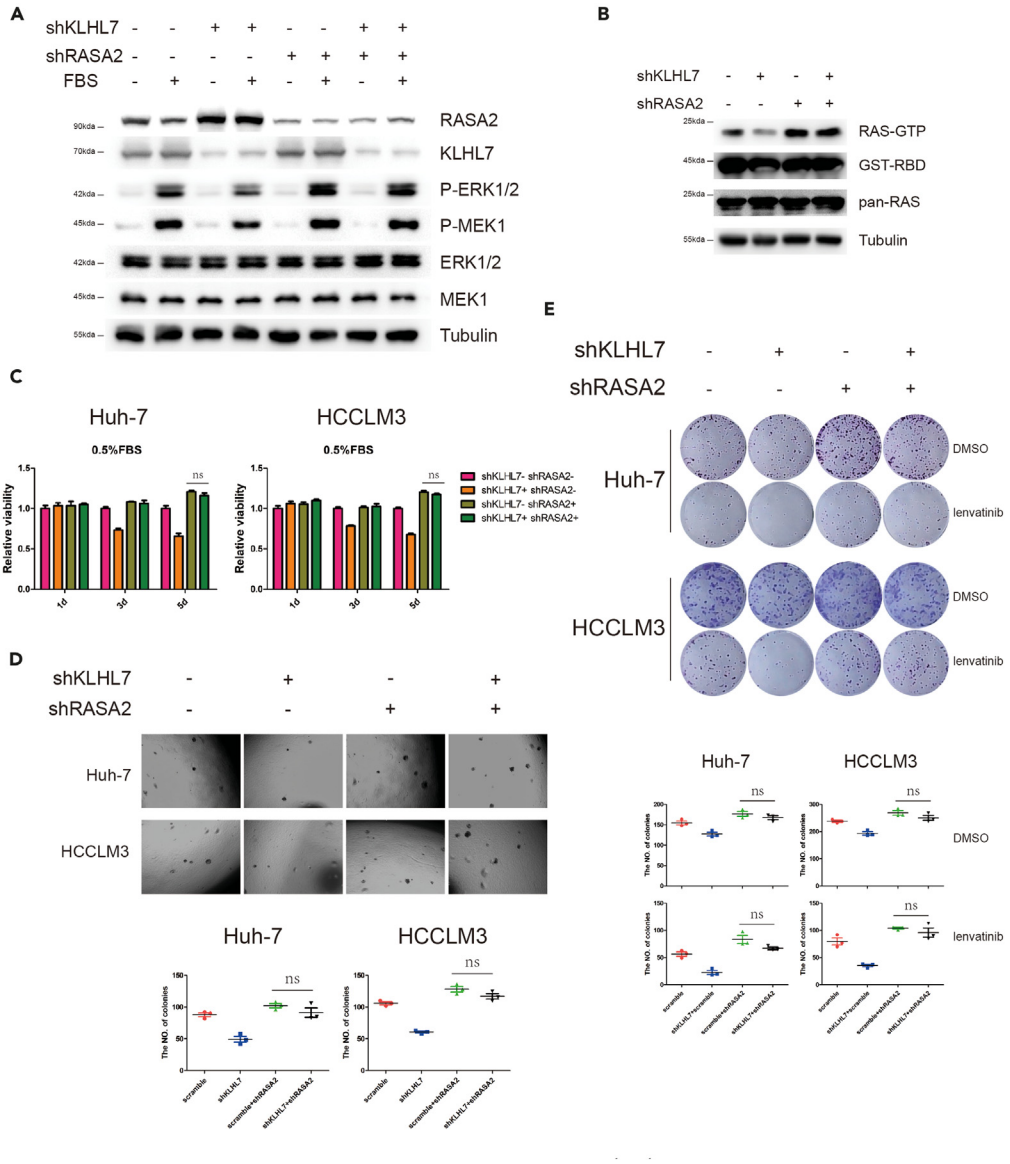

Figure 5. KLHL7 upregulates the RAS-MAPK pathway via RASA2

(A) Huh-7 cells were transfected with the corresponding shRNA, starved for 16 h before being stimulated with FBS for 15 min, and lysed for immunoblotting.

(B) Serum-starved Huh-7 cells transfected with the indicated shRNA were triggered with FBS for 5 min and lysed for GST-RAS-RBD pulldown. The pulldown protein was detected by immunoblotting.

(C) Cell viability assays were performed with cells transfected with the indicated shRNA in media containing 0.5% fetal bovine serum. The cell number was detected by adding CCK-8 and measuring the absorbance at 450 nM. Data are the mean ± s.e.m. n = 4. Significance was determined using Student's *t* test. ns $p > 0.05$.

(D) A soft agar formation assay was performed with cells transfected with the indicated shRNA. Data are the mean ± s.e.m. n = 3. Significance was determined using Student's *t* test. ns $p > 0.05$.

(E) Colony formation assays were performed on cells transfected with the indicated shRNA after 2 weeks of lenvatinib treatment. The statistics of the number of remaining clones are shown at the bottom. Lenvatinib concentrations were 0.5 μM (Huh-7) and 1 μM (HCCLM3). Data are the mean ± s.e.m. n = 3. Significance was determined using Student's *t* test. ns $p > 0.05$.

In addition, we revealed *in vitro* that chemoresistance induced by KLHL7 exists in a RASA2-dependent manner. When both KLHL7 and RASA2 were knocked down, the number of lenvatinib-resistant clones was largely unchanged compared to when RASA2 was knocked down alone (Figure 5E).

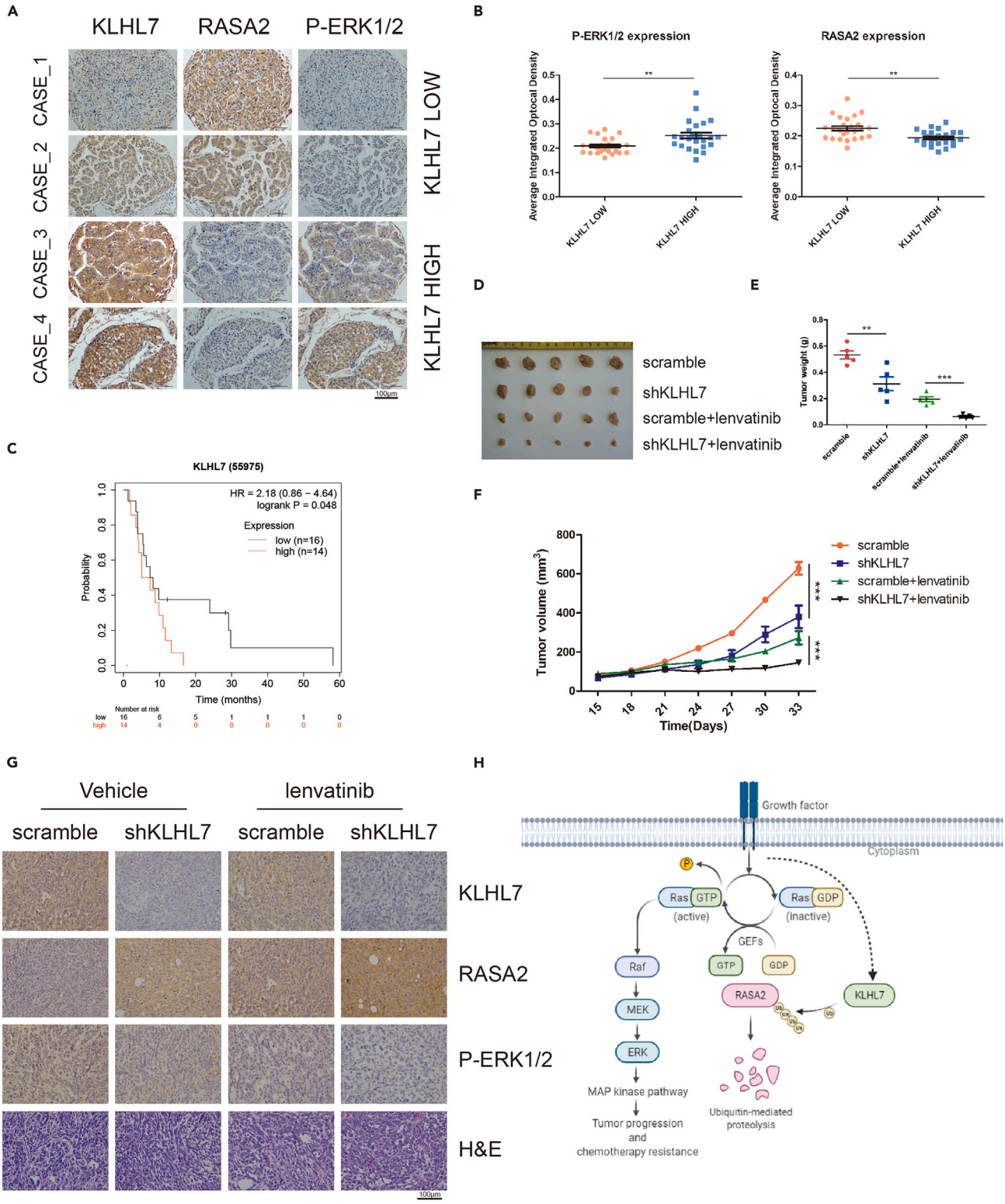

Figure 6. KLHL7 knockdown makes hepatocellular carcinoma susceptible to lenvatinib *in vivo*

(A and B) Detection of the expression of the indicated proteins in HCC tissue by immunohistochemistry. A, Immunohistochemical images. Image magnification is 20×. Scale bar, 100 μm. B, The expression of P-ERK1/2 and RASA2 in the KLHL7 low-expression group and KLHL7 high-expression group.

Figure 6. *Continued*

Expression intensity was determined by measuring the average optical density. Data are the mean ± s.e.m. n = 25. Significance was determined using Student's *t* test. **p < 0.01.

(C) Overall survival curve of 30 HCC patients who received sorafenib treatment. According to the best cutoff by the system, 16 patients were assigned to the KLHL7 low-expression group and 14 patients were assigned to the KLHL7 high-expression group. (data from http://kmplot.com/analysis/).

(D and G) Knockdown KLHL7 and control HCCLM3 cells were subjected to subcutaneous tumorigenesis in nude mice and treated with oral lenvatinib. (D), Images of the tumors at the end of the experiment. Image magnification is 20×. Scale bar, 100 μm. (E). Weight of the tumor at the end of the experiment. (F), Growth curve of tumors. (G). Immunohistochemical staining of the indicated proteins and H&E staining images of the tumor at the end of the experiment.

(H) An overview of the entire article.

In vivo inhibition of klhl7 increases the efficacy of molecular therapy for hepatocellular carcinoma

To further confirm our hypothesis, we evaluated the association of KLHL7 expression with RASA2 and ERK activation in HCC tissues through immunohistochemistry (Figure S5A). Based on KLHL7 expression, tumor tissues were divided into low-expression and high-expression groups. RASA2 expression was significantly lower in the high-KLHL7 expression group compared to the low-KLHL7 expression group, whereas phosphorylation of ERK1/2 was higher (Figures 6A and 6B). We observed a negative correlation between KLHL7 expression and RASA2 expression and a positive correlation with ERK1/2 phosphorylation (Figures S5B and S5C).

In vitro studies have shown that KLHL7 is an oncogene in HCC and that it affects the response of HCC cells to molecular therapy. Moreover, we found that sorafenib-treated HCC patients with high-KLHL7 mRNA expression showed worse progression-free survival than those with low-KLHL7 expression (Figure 6C). These results suggested that KLHL7 may be a potential target for the treatment of HCC. To test this hypothesis, we used the HCCLM3 cell line to establish a subcutaneous xenograft tumor model and administered lenvatinib. Similar to the Huh-7-cell line, KLHL7 knockdown inhibited tumor growth in HCCLM3 cells. The combination of KLHL7 knockdown with lenvatinib treatment accelerated tumor volume reduction compared to lenvatinib administration alone (Figures 6D–6F).

We also detected the expression of KLHL7, RASA2, and phosphorylated ERK1/2 in xenograft tumors by immunohistochemistry. Lenvatinib treatment significantly decreased the phosphorylation level of ERK1/2 *in vivo, and* shRNA was still able to effectively knockdown KLHL7. Consistent with our hypothesis (Figure 6H), KLHL7 knockdown increased the RASA2 protein level and inhibited ERK1/2 phosphorylation (Figure 6G). Our *in vivo* experiments confirmed that KLHL7 regulated RASA2 indicating that KLHL7 could be a potential therapeutic target for the treatment of HCC.

DISCUSSION

The role of KLHL7 in tumors is rarely reported. As an adapter for the BTB-CUL3-RBX1 E3 ubiquitination ligase, KLHL7 primarily complements the ubiquitination modification of substrates by binding to CUL3 through its BTB domain.[21,39] Tumor suppressor genes, such as KEAP1[40] and LZTR1,[41] and oncogenes, such as KBTBD6/7[42] and KLHL22,[43] are examples of proteins containing BTB domains. In a recent study on breast cancer, KLHL7 was identified as a marker of poor prognosis.[44] In HCC, we also found that elevated KLHL7 expression suggested a poor prognosis. We found that KLHL7 can interact with RASA2, confirming the bioplex database results.[34,35] Previous reports indicate that KLHL7 is mainly involved in K48-linked ubiquitination,[21] while our findings imply that KLHL7 modifies and degrades the RASA2 protein via K48-linked polyubiquitination.

Numerous studies in HCC have demonstrated multiple mechanisms leading to dysregulated MAPK-RAS activity. It has been reported that members of the Ras association domain family, including RASSF1 and RASSF5, are down-regulated in HCC and are associated with sensitivity to sorafenib treatment.[45,46] The epigenetic silencing of RAS GAPs, such as RASAL1, DAB2IP, or NF1, increased HCC proliferation and resistance to apoptosis.[47] RASA2 belongs to the RAS GAPs, and its inactivating mutation is considered a driver of melanoma.[15] Our research suggests that the RAS-MAPK signaling pathway is regulated by the stability of the RASA2 protein, which decreases in response to growth factor stimulation. In response to growth factor signals, cells upregulate KLHL7 and degrade RASA2, ensuring the efficiency and specificity of signaling within the RAS-MAPK cascade.

The RAS-MAPK pathway is one of the most frequently mutated pathways in human tumors. Mutations in this signaling pathway, however, are uncommon in HCC, which is driven by multiple genes. Thus, there are no effective treatments for HCC. Sorafenib and lenvatinib are multikinase inhibitors and remain the first-line treatment in the clinic but have very poor therapeutic effects. Inhibition of KLHL7 by shRNA transfection significantly enhanced HCC cell responsiveness to lenvatinib, suggesting that KLHL7 could be a potential therapeutic target for HCC therapy.

Limitations of the study

In this study, we found that serum stimulation after cell starvation resulted in increased KLHL7 expression and decreased RASA2 expression. The detailed mechanism still remains to be further investigated.

STAR★METHODS

Detailed methods are provided in the online version of this paper and include the following:

- KEY RESOURCES TABLE
- RESOURCE AVAILABILITY
  - Lead contact
  - Material availability
  - Data and code availability
- EXPERIMENTAL MODEL AND SUBJECT DETAILS
- METHOD DETAILS
  - Cell lines and transfections
  - Plasmid
  - Patient specimens and tissue microarrays
  - Antibodies and chemicals
  - Ubiquitination assay
  - GST-RAF1 RBD pulldown
  - Colony formation assays
  - The soft agar colony formation assay
  - Cell viability assays
  - Real-time PCR
  - Immunofluorescence
- QUANTIFICATION AND STATISTICAL ANALYSIS
- ADDITIONAL RESOURCES

SUPPLEMENTAL INFORMATION

Supplemental information can be found online at https://doi.org/10.1016/j.isci.2023.106914.

ACKNOWLEDGMENTS

This work was supported by the National Natural Science Foundation of China (grants 81570537, 81974074 and 82172654).

AUTHOR CONTRIBUTIONS

L.C. and Y.L. designed the study. L.C. performed experiments, analyzed the samples, and interpreted the results. L.C. and Y.L. wrote the manuscript. All authors reviewed and approved the manuscript before submission.

DECLARATION OF INTERESTS

The authors declare no competing interests.

Received: September 25, 2022
Revised: December 27, 2022
Accepted: May 14, 2023
Published: May 19, 2023

REFERENCES

1. Sung, H., Ferlay, J., Siegel, R.L., Laversanne, M., Soerjomataram, I., Jemal, A., and Bray, F. (2021). Global cancer statistics 2020: GLOBOCAN estimates of incidence and mortality worldwide for 36 cancers in 185 countries. CA A Cancer J. Clin. *71*, 209–249. https://doi.org/10.3322/caac.21660.

2. Cancer Genome Atlas Research Network Electronic address wheeler@bcmedu; Cancer Genome Atlas Research Network; Electronic address, w.b.e.; Cancer Genome Atlas Research, N (2017). Comprehensive and Integrative Genomic Characterization of Hepatocellular Carcinoma. Cell *169*, 1327–1341.e23. https://doi.org/10.1016/j.cell.2017.05.046.

3. Llovet, J.M., Kelley, R.K., Villanueva, A., Singal, A.G., Pikarsky, E., Roayaie, S., Lencioni, R., Koike, K., Zucman-Rossi, J., and Finn, R.S. (2021). Hepatocellular carcinoma. Nat. Rev. Dis. Prim. *7*, 6. https://doi.org/10.1038/s41572-020-00240-3.

4. Finn, R.S., and Zhu, A.X. (2021). Evolution of systemic therapy for hepatocellular carcinoma. Hepatology *73* (*Suppl 1*), 150–157. https://doi.org/10.1002/hep.31306.

5. Finn, R.S., Qin, S., Ikeda, M., Galle, P.R., Ducreux, M., Kim, T.Y., Kudo, M., Breder, V., Merle, P., Kaseb, A.O., et al. (2020). Atezolizumab plus bevacizumab in unresectable hepatocellular carcinoma. N. Engl. J. Med. *382*, 1894–1905. https://doi.org/10.1056/NEJMoa1915745.

6. Llovet, J.M., Ricci, S., Mazzaferro, V., Hilgard, P., Gane, E., Blanc, J.F., de Oliveira, A.C., Santoro, A., Raoul, J.L., Forner, A., et al. (2008). Sorafenib in advanced hepatocellular carcinoma. N. Engl. J. Med. *359*, 378–390. https://doi.org/10.1056/NEJMoa0708857.

7. Kudo, M., Finn, R.S., Qin, S., Han, K.H., Ikeda, K., Piscaglia, F., Baron, A., Park, J.W., Han, G., Jassem, J., et al. (2018). Lenvatinib versus sorafenib in first-line treatment of patients with unresectable hepatocellular carcinoma: a randomised phase 3 non-inferiority trial. Lancet *391*, 1163–1173. https://doi.org/10.1016/S0140-6736(18)30207-1.

8. Dhillon, A.S., Hagan, S., Rath, O., and Kolch, W. (2007). MAP kinase signalling pathways in cancer. Oncogene *26*, 3279–3290. https://doi.org/10.1038/sj.onc.1210421.

9. Zhang, W., and Liu, H.T. (2002). MAPK signal pathways in the regulation of cell proliferation in mammalian cells. Cell Res. *12*, 9–18. https://doi.org/10.1038/sj.cr.7290105.

10. Huang, S., Hölzel, M., Knijnenburg, T., Schlicker, A., Roepman, P., McDermott, U., Garnett, M., Grernrum, W., Sun, C., Prahallad, A., et al. (2012). MED12 controls the response to multiple cancer drugs through regulation of TGF-beta receptor signaling. Cell *151*, 937–950. https://doi.org/10.1016/j.cell.2012.10.035.

11. Jin, H., Shi, Y., Lv, Y., Yuan, S., Ramirez, C.F.A., Lieftink, C., Wang, L., Wang, S., Wang, C., Dias, M.H., et al. (2021). EGFR activation limits the response of liver cancer to lenvatinib. Nature *595*, 730–734. https://doi.org/10.1038/s41586-021-03741-7.

12. Downward, J. (2003). Targeting RAS signalling pathways in cancer therapy. Nat. Rev. Cancer *3*, 11–22. https://doi.org/10.1038/nrc969.

13. Karnoub, A.E., and Weinberg, R.A. (2008). Ras oncogenes: split personalities. Nat. Rev. Mol. Cell Biol. *9*, 517–531. https://doi.org/10.1038/nrm2438.

14. Aoki, Y., Niihori, T., Inoue, S.i., and Matsubara, Y. (2016). Recent advances in RASopathies. J. Hum. Genet. *61*, 33–39. https://doi.org/10.1038/jhg.2015.114.

15. Arafeh, R., Qutob, N., Emmanuel, R., Keren-Paz, A., Madore, J., Elkahloun, A., Wilmott, J.S., Gartner, J.J., Di Pizio, A., Winograd-Katz, S., et al. (2015). Recurrent inactivating RASA2 mutations in melanoma. Nat. Genet. *47*, 1408–1410. https://doi.org/10.1038/ng.3427.

16. Brems, H., Chmara, M., Sahbatou, M., Denayer, E., Taniguchi, K., Kato, R., Somers, R., Messiaen, L., De Schepper, S., Fryns, J.P., et al. (2007). Germline loss-of-function mutations in SPRED1 cause a neurofibromatosis 1-like phenotype. Nat. Genet. *39*, 1120–1126. https://doi.org/10.1038/ng2113.

17. Revencu, N., Boon, L.M., Mendola, A., Cordisco, M.R., Dubois, J., Clapuyt, P., Hammer, F., Amor, D.J., Irvine, A.D., Baselga, E., et al. (2013). RASA1 mutations and associated phenotypes in 68 families with capillary malformation-arteriovenous malformation. Hum. Mutat. *34*, 1632–1641. https://doi.org/10.1002/humu.22431.

18. Simanshu, D.K., Nissley, D.V., and McCormick, F. (2017). RAS proteins and their regulators in human disease. Cell *170*, 17–33. https://doi.org/10.1016/j.cell.2017.06.009.

19. Deshaies, R.J., and Joazeiro, C.A.P. (2009). RING domain E3 ubiquitin ligases. Annu. Rev. Biochem. *78*, 399–434. https://doi.org/10.1146/annurev.biochem.78.101807.093809.

20. Petroski, M.D., and Deshaies, R.J. (2005). Function and regulation of cullin-RING ubiquitin ligases. Nat. Rev. Mol. Cell Biol. *6*, 9–20. https://doi.org/10.1038/nrm1547.

21. Kigoshi, Y., Tsuruta, F., and Chiba, T. (2011). Ubiquitin ligase activity of Cul3-KLHL7 protein is attenuated by autosomal dominant retinitis pigmentosa causative mutation. J. Biol. Chem. *286*, 33613–33621. https://doi.org/10.1074/jbc.M111.245126.

22. Angius, A., Uva, P., Buers, I., Oppo, M., Puddu, A., Onano, S., Persico, I., Loi, A., Marcia, L., Höhne, W., et al. (2016). Bi-Allelic mutations in KLHL7 cause a crisponi/CISS1-like phenotype associated with early-onset retinitis pigmentosa. Am. J. Hum. Genet. *99*, 236–245. https://doi.org/10.1016/j.ajhg.2016.05.026.

23. Chandrashekar, D.S., Bashel, B., Balasubramanya, S.A.H., Creighton, C.J., Ponce-Rodriguez, I., Chakravarthi, B.V.S.K., and Varambally, S. (2017). UALCAN: a portal for facilitating tumor subgroup gene expression and survival analyses. Neoplasia *19*, 649–658. https://doi.org/10.1016/j.neo.2017.05.002.

24. Lánczky, A., and Győrffy, B. (2021). Web-Based survival analysis tool tailored for medical research (KMplot): development and implementation. J. Med. Internet Res. *23*, e27633. https://doi.org/10.2196/27633.

25. Tomczak, K., Czerwińska, P., and Wiznerowicz, M. (2015). The Cancer Genome Atlas (TCGA): an immeasurable source of knowledge. Contemp. Oncol. *19*, A68–A77. https://doi.org/10.5114/wo.2014.47136.

26. Castel, P., Cheng, A., Cuevas-Navarro, A., Everman, D.B., Papageorge, A.G., Simanshu, D.K., Tankka, A., Galeas, J., Urisman, A., and McCormick, F. (2019). RIT1 oncoproteins escape LZTR1-mediated proteolysis. Science *363*, 1226–1230. https://doi.org/10.1126/science.aav1444.

27. Yu, F.X., Zhao, B., Panupinthu, N., Jewell, J.L., Lian, I., Wang, L.H., Zhao, J., Yuan, H., Tumaneng, K., Li, H., et al. (2012). Regulation of the Hippo-YAP pathway by G-protein-coupled receptor signaling. Cell *150*, 780–791. https://doi.org/10.1016/j.cell.2012.06.037.

28. Riecken, L.B., Tawamie, H., Dornblut, C., Buchert, R., Ismayel, A., Schulz, A., Schumacher, J., Sticht, H., Pohl, K.J., Cui, Y., et al. (2015). Inhibition of RAS activation due to a homozygous ezrin variant in patients with profound intellectual disability. Hum. Mutat. *36*, 270–278. https://doi.org/10.1002/humu.22737.

29. Brtva, T.R., Drugan, J.K., Ghosh, S., Terrell, R.S., Campbell-Burk, S., Bell, R.M., and Der, C.J. (1995). Two distinct Raf domains mediate interaction with Ras. J. Biol. Chem. *270*, 9809–9812. https://doi.org/10.1074/jbc.270.17.9809.

30. Brummelkamp, T.R., Bernards, R., and Agami, R. (2002). Stable suppression of tumorigenicity by virus-mediated RNA interference. Cancer Cell *2*, 243–247. https://doi.org/10.1016/s1535-6108(02)00122-8.

31. Catling, A.D., Schaeffer, H.J., Reuter, C.W., Reddy, G.R., and Weber, M.J. (1995). A proline-rich sequence unique to MEK1 and MEK2 is required for raf binding and regulates MEK function. Mol. Cell Biol. *15*, 5214–5225. https://doi.org/10.1128/MCB.15.10.5214.

32. Wang, T., Yu, H., Hughes, N.W., Liu, B., Kendirli, A., Klein, K., Chen, W.W., Lander, E.S., and Sabatini, D.M. (2017). Gene essentiality profiling reveals gene networks and synthetic lethal interactions with oncogenic Ras. Cell *168*, 890–903.e15. https://doi.org/10.1016/j.cell.2017.01.013.

33. Welchman, R.L., Gordon, C., and Mayer, R.J. (2005). Ubiquitin and ubiquitin-like proteins as multifunctional signals. Nat. Rev. Mol. Cell Biol. *6*, 599–609. https://doi.org/10.1038/nrm1700.

34. Huttlin, E.L., Ting, L., Bruckner, R.J., Gebreab, F., Gygi, M.P., Szpyt, J., Tam, S., Zarraga, G., Colby, G., Baltier, K., et al. (2015). The BioPlex network: a systematic exploration of the human interactome. Cell *162*, 425–440. https://doi.org/10.1016/j.cell.2015.06.043.

35. Huttlin, E.L., Bruckner, R.J., Paulo, J.A., Cannon, J.R., Ting, L., Baltier, K., Colby, G., Gebreab, F., Gygi, M.P., Parzen, H., et al. (2017). Architecture of the human interactome defines protein communities and disease networks. Nature *545*, 505–509. https://doi.org/10.1038/nature22366.

36. Kim, J.H., Chang, T.M., Graham, A.N., Choo, K.H.A., Kalitsis, P., and Hudson, D.F. (2010). Streptavidin-Binding Peptide (SBP)-tagged SMC2 allows single-step affinity fluorescence, blotting or purification of the condensin complex. BMC Biochem. *11*, 50. https://doi.org/10.1186/1471-2091-11-50.

37. Lim, K.L., Chew, K.C.M., Tan, J.M.M., Wang, C., Chung, K.K.K., Zhang, Y., Tanaka, Y., Smith, W., Engelender, S., Ross, C.A., et al. (2005). Parkin mediates nonclassical, proteasomal-independent ubiquitination of synphilin-1: implications for Lewy body formation. J. Neurosci. *25*, 2002–2009. https://doi.org/10.1523/JNEUROSCI.4474-04.2005.

38. Pintard, L., Willems, A., and Peter, M. (2004). Cullin-based ubiquitin ligases: cul3-BTB complexes join the family. EMBO J. *23*, 1681–1687. https://doi.org/10.1038/sj.emboj.7600186.

39. Wang, P., Song, J., and Ye, D. (2020). CRL3s: the BTB-CUL3-RING E3 ubiquitin ligases. Adv. Exp. Med. Biol. *1217*, 211–223. https://doi.org/10.1007/978-981-15-1025-0_13.

40. Kansanen, E., Kuosmanen, S.M., Leinonen, H., and Levonen, A.L. (2013). The Keap1-Nrf2 pathway: mechanisms of activation and dysregulation in cancer. Redox Biol. *1*, 45–49. https://doi.org/10.1016/j.redox.2012.10.001.

41. Bigenzahn, J.W., Collu, G.M., Kartnig, F., Pieraks, M., Vladimer, G.I., Heinz, L.X., Sedlyarov, V., Schischlik, F., Fauster, A., Rebsamen, M., et al. (2018). LZTR1 is a regulator of RAS ubiquitination and signaling. Science *362*, 1171–1177. https://doi.org/10.1126/science.aap8210.

42. Genau, H.M., Huber, J., Baschieri, F., Akutsu, M., Dötsch, V., Farhan, H., Rogov, V., and Behrends, C. (2015). CUL3-KBTBD6/KBTBD7 ubiquitin ligase cooperates with GABARAP proteins to spatially restrict TIAM1-RAC1 signaling. Mol. Cell *57*, 995–1010. https://doi.org/10.1016/j.molcel.2014.12.040.

43. Chen, J., Ou, Y., Yang, Y., Li, W., Xu, Y., Xie, Y., and Liu, Y. (2018). KLHL22 activates amino-acid-dependent mTORC1 signalling to promote tumorigenesis and ageing. Nature *557*, 585–589. https://doi.org/10.1038/s41586-018-0128-9.

44. Kurozumi, S., Joseph, C., Sonbul, S., Gorringe, K.L., Pigera, M., Aleskandarany, M.A., Diez-Rodriguez, M., Nolan, C.C., Fujii, T., Shirabe, K., et al. (2018). Clinical and biological roles of Kelch-like family member 7 in breast cancer: a marker of poor prognosis. Breast Cancer Res. Treat. *170*, 525–533. https://doi.org/10.1007/s10549-018-4777-z.

45. Azumi, J., Tsubota, T., Sakabe, T., and Shiota, G. (2016). miR-181a induces sorafenib resistance of hepatocellular carcinoma cells through downregulation of RASSF1 expression. Cancer Sci. *107*, 1256–1262. https://doi.org/10.1111/cas.13006.

46. Delire, B., and Stärkel, P. (2015). The Ras/MAPK pathway and hepatocarcinoma: pathogenesis and therapeutic implications. Eur. J. Clin. Invest. *45*, 609–623. https://doi.org/10.1111/eci.12441.

47. Newell, P., Toffanin, S., Villanueva, A., Chiang, D.Y., Minguez, B., Cabellos, L., Savic, R., Hoshida, Y., Lim, K.H., Melgar-Lesmes, P., et al. (2009). Ras pathway activation in hepatocellular carcinoma and anti-tumoral effect of combined sorafenib and rapamycin in vivo. J. Hepatol. *51*, 725–733. https://doi.org/10.1016/j.jhep.2009.03.028.

STAR★METHODS

KEY RESOURCES TABLE

REAGENT or RESOURCE	SOURCE	IDENTIFIER
Antibodies		
Anti-KLHL7 (kelch-like family member 7)	Sigma-Aldrich	Cat#HPA029491; RRID:AB_10599605
RASA2 Rabbit pAb	ABclonal	Cat#A18375; RRID:AB_2862142
Phospho-p44/42 MAPK (Erk1/2) (Thr202/Tyr204) Antibody	Cell Signaling Technology	Cat#4376; RRID:AB_331772
Phospho-MEK1/2 (Ser217/221) (41G9) Rabbit mAb	Cell Signaling Technology	Cat#9154; RRID:AB_2138017
p44/42 MAPK (Erk1/2) Antibody	Cell Signaling Technology	Cat#3510; RRID:AB_1595393
MEK1/2 Antibody	Cell Signaling Technology	Cat#9122; RRID:AB_823567
KRAS+HRAS+NRAS Rabbit mAb	ABclonal	Cat#A19779; RRID:AB_2862751
Monoclonal ANTI-FLAG(R) M2 antibody produced in mouse	Sigma-Aldrich	Cat#F4049; RRID:AB_439701
DYKDDDDK Tag (D6W5B) Rabbit mAb (Binds to same epitope as Sigma's Anti-FLAG ® M2 Antibody)	Cell Signaling Technology	Cat#70569; RRID:AB_2799786
Mouse anti Myc-Tag mAb	Abclonal	Cat#AE010; RRID:AB_2770408
HA-Tag(26D11) mAb	Abmart	Cat#M20003; RRID:AB_2864345
GST-Tag(12G8) mAb	Abmart	Cat#M20007; RRID:AB_2864360
Biological samples		
Tissue Micriarray 1	SHANGHAI OUTDO BIOTECH	Cat#HLiv-HCC030PG-01
Tissue Micriarray 2	SHANGHAI OUTDO BIOTECH	Cat#HLiv-SP041
Chemicals, peptides, and recombinant proteins		
MG132	Selleck	Cat#S2619
Cycloheximide (NSC-185)	Selleck	Cat#S7418
Streptavidin Agarose Resin 6FF	YEASEN	Cat#20512ES08
Matrigel® Basement Membrane Matrix	Corning	Cat#356234
GSTSep Glutathione Agarose Resin 4FF	YEASEN	Cat#20508ES10
Lenvatinib mesylate	GLPBIO	Cat#GC36438
Sorafenib Tosylate	GLPBIO	Cat#GC16499
Experimental models: Cell lines		
Hep3B	Procell. China	Cat#CL-0102
HepG2	Procell. China	Cat#CL-0103
Huh-7	Procell. China	Cat#CL-0120
HCCLM3	Qiao Xin Zhou Biotechnology	Cat#ZQ0023
HEK293T	Chinese Academy of Sciences	Cat#SCSP-502
Experimental models: Organisms/strains		
BALB/c nude Mice	Charles River	Cat#194
Oligonucleotides		
shKLHL7(1): TCATCAGTGAAGCGCAGTATC	This paper	N/A
shKLHL7(2): CTGCTAGAATTTCCGTGAATA	This paper	N/A
shRASA2: GAATCTGCGCTACTATGTAGA	This paper	N/A
ACTB Forward: GCTCCGGCATGTGCAAGG	This paper	N/A
ACTB Reverse: GGCCTCGTCGCCCACATA	This paper	N/A

(*Continued on next page*)

Continued

REAGENT or RESOURCE	SOURCE	IDENTIFIER
KLHL7 Forward: CATCGTGTTGTTCTTGCTGC	This paper	N/A
KLHL7 Reverse: AGCAAATTCCACCAGTTGTTC	This paper	N/A
RASA2 Forward: GCTGTTTTGCCCCTTGTACG	This paper	N/A
RASA2 Reverse: ATCCAGACATCGGGTAGCCA	This paper	N/A
Recombinant DNA		
pcDNA3.1 (+)	Invitrogen	Cat#V79020
pLKO.1 puro	addgene	Plasmid #8453
pMD2.G	addgene	Plasmid #12259
psPAX2	addgene	Plasmid #12260
pRK5-HA-Ubiquitin-WT	addgene	Plasmid #17608
pRK5-HA-Ubiquitin-K63	addgene	Plasmid #17606
pRK5-HA-Ubiquitin-K48	addgene	Plasmid #17605
Raf-1 GST RBD 1-149	addgene	Plasmid #13338
pLKO.1-blast	addgene	Plasmid #26655
pLVX-IRES-Puro(Flag-SBP)	This paper	N/A
pLV-Ubc-MCS-IRES-Bsd	This paper	N/A
Software and algorithms		
Image-Pro Plus	Media Cy	https://www.mediacy.com/78-products/image-pro-plus
Prism	GraphPad	https://www.graphpad.com/scientific-software/prism/

RESOURCE AVAILABILITY

Lead contact

Further information and requests for resources should be directed to and will be fulfilled by the lead contact, Yongheng Chen, yonghenc@csu.edu.cn.

Material availability

Further information and requests for resources and reagents should be directed to and will be fulfilled by the lead contact.

Data and code availability

- The data presented in this study are available on request from the lead contact upon request.
- This paper does not report original code.
- Any additional data supporting findings on this study are available from the lead contact upon request.

EXPERIMENTAL MODEL AND SUBJECT DETAILS

6 week-old male BALB/c nude mice were purchased from the SLAC Jingda Laboratory Animal Co.Ltd (Hunan, China). All animal experiments were performed under specific sterile barrier conditions. All protocols were approved by the Animal Ethics Committee (No. 2021049). A total of 5×10^6 cells resuspended in 100 μL of Matrigel were subcutaneously transplanted into nude mice. Lenvatinib (10 mg/kg) was administered orally 5 times a week when the tumors reached approximately 100 mm^3. Tumors were measured every 3 days, and tumor volume was determined using the formula length*width^2/2. 293T cell line was obtained from the Chinese Academy of Sciences (Shanghai, China). Huh-7 and Hep3B were purchased from Procell (Wuhan, China). HCCLM3 was purchased from the Zhong Qiao Xin Zhou Biotechnology (Shanghai, China).The companies have authenticated these cell lines and test these cell line for mycoplasma prior to sale.

METHOD DETAILS

Cell lines and transfections

Hepatocellular carcinoma cell lines were grown in DMEM containing 10% fetal bovine serum (Newzerum) at 37°C in a humidified incubator with 95% air and 5% CO2. jetOPTIMUS (Polyplus) was the reagent used for the transfection of plasmids.

Plasmid

The pLV-Ubc-MCS-IRES-Bsd and PCDNA3.1 plasmids were used for gene expression. The pLV-Ubc-MCS-IRES-Bsd plasmid is used to rebuild KLHL7 expression. The shRNA lentiviral vectors were pLKO.1-puro and pLKO.1-bsd. pMD2. G (Addgene) and psPAX2 (Addgene) plasmids were used as helper packing plasmids for lentiviral production. ShRNA sequences for KLHL7 were as follows: 1, TCATCAGTGAAGCGCAGTATC (3′UTR); 2, CTGCTAGAATTTCCGTGAATA(CDS). shRNA sequence for RASA2: GAATCTGCGCTACTATGTAGA. MEK1CA is the MEK1 mutation consisting of 218 and 222 S to D.

Patient specimens and tissue microarrays

Tissue chips comprising HCC tissue samples and adjacent nontumoral tissues were purchased from Shanghai Outdo Biotech Company, Shanghai, China. Tissue microarray chips contained HCC tissues and adjacent nontumoral liver tissues from 15 patients to detect KLHL7 expression. Another chip contains 50 HCC tissues to detect the expression of KLHL7, RASA2, and P-ERK1/2 in hepatocellular carcinoma. Immunohistochemistry was performed with the following primary antibodies: KLHL7 (Atlas Antibodies HPA029491, 1:100); RASA2 (Abclonal, A18375. 1:100); and P-ERK1/2 (Cell Signaling Technology, 4376, 1:50). The protein expression intensity was measured by analyzing the mean optical density using Image-Pro Plus software.

Antibodies and chemicals

The following antibodies were used for western blotting: KLHL7 (Atlas Antibodies HPA029491, 1:1000); RASA2 (Abclonal, A18375, 1:1000); P-ERK1/2 (Cell Signaling Technology, 4376, 1:1000); P-MEK1/2 (Cell Signaling Technology, 9154, 1:500); ERK1/2 (Cell Signaling Technology, 9102, 1:500); MEK1/2 (Cell Signaling Technology, 9122, 1:1000); pan-RAS (Abclonal, A19779, 1:1000); FLAG (Milliporesigma, F3165, 1:4000; Cell Signaling Technology, 14793, 1:4000); myc-tag (Abclonal, AE010, 1:4000); HA-tag(Abmart, M20003, 1:4000) and GST-tag (Abmart, M20007, 1:4000). Both MG-132 and CHX were purchased from Selleck.

Ubiquitination assay

The HA-Ubiqitin expressing plasmids were purchased from Addgene (17608, 17606, 17605). The HA-Ubiqitin-expressing vector and other expression vectors were transiently cotransfected into 293T cells using jetOPTIMUS (Polyplus). Forty-eight hours later, 293T cells were lysed using immunoprecipitation buffer (50 mM Tris, pH 7.4, 200 mM NaCl, 1% Triton X-100, protease inhibitor cocktail). Proteins that require detection of ubiquitination modification levels are SBP-tagged and enriched by streptavidin beads. The level of ubiquitination modification was detected by western blotting using an antibody against the HA tag.

GST-RAF1 RBD pulldown

The prokaryotic plasmid expressing the GST-RAF1 RBD was purchased from Addgene (13338). Hepatoma cells were stimulated with fetal bovine serum (FBS) for 5 min and then lysed in immunoprecipitation buffer (50 mM Tris, pH 7.4, 200 mM NaCl, 1% Triton X-100, protease inhibitor cocktail). Cell lysates were incubated with GST-RBD (10 μg) at 4°C for 60 min, and then to enrich GTP-bound RAS by GST Agarose Beads. GTP-bound RAS proteins were detected by Western blotting using an antibody against pan-RAS.

Colony formation assays

The indicated tumor cells were seeded in 12-well plates (1000 cells per well) and then treated with therapeutic agents for 2 weeks. The colonies were fixed with 100% methanol for 30 min and stained with 0.1% crystal violet.

The soft agar colony formation assay

As the bottom layer, 300 μL of DMEM complete medium containing 0.6% low melting point agar was injected into a 24-well plate. After the bottom layer had solidified, 2000 hepatoma cells were mixed with

300 μL DMEM complete media containing 0.35% low melting point agar and injected into the wells. After 3 weeks of cell growth in soft agar, the number of colonies in each well was determined using a light microscope.

Cell viability assays

Cells were seeded in 96-well plates. During testing, the medium was aspirated and replaced with fresh media containing 10% CCK-8, which was incubated for 30 minutes. The absorbance was measured at a wavelength of 450 nm. Cell viability= $(OD_{treatment}-OD_{blank})/(OD_{control}-OD_{blank})$.

Real-time PCR

RNA was extracted using TRIzol Reagent (Invitrogen). Reverse transcription reagents and qPCR mix were purchased from Vazyme. The PCR primers were ACTB, F: GCTCCGGCATGTGCAAGG, R: GGCCT CGTCGCCCACATA; KLHL7, F: CATCGTGTTGTTCTTGCTGC, R: AGCAAATTCCACCAGTTGTTC; and RASA2, F: GCTGTTTTGCCCCTTGTACG, R: ATCCAGACATCGGGTAGCCA.

Immunofluorescence

Cells were grown in chamber slides and were fixed by formaldehyde solution for 15 min. After rinsing 3 times, the cells were blocked and permeabilized by blocking buffer (1X PBS/5% BSA/0.3% Triton X-100) for 60 min. The blocking buffer was aspirated, followed by incubation with diluted primary antibody overnight at 4°C. Samples were rinsed three times in PBS for 5 min, and incubated with secondary antibody for 1 h at room temperature in the dark. After rinsing three times in PBS, samples were stained with DAPI (Solebro, C0065) and collected under a Zeiss microscope. Immunofluorescence was performed with the following antibodies: KLHL7 (Atlas Antibodies HPA029491, 1:100); FLAG (Milliporesigma, F3165, 1:250).

QUANTIFICATION AND STATISTICAL ANALYSIS

Statistical analyses were performed using GraphPad Prism software. Differences between groups were analyzed by Student's *t* test. The results of quantitative data in histograms were presented as mean ± SEM and the data were considered significant when $p < 0.05$. The meaning of asterisks number were *$p < 0.05$, **$p < 0.01$, ***$p < 0.001$, and ns means not significant.

ADDITIONAL RESOURCES

Clinical patient samples and patient information related to this study were collected by Shanghai Outdo Biotech Company. All actions were approved by its ethics committee (No. SHXC2021YF01).